ELSEVIER

FEMS Microbiology Ecology 44 (2003) 203–215

FEMS MICROBIOLOGY Ecology

www.fems-microbiology.org

Spatial distribution of bacterial communities and their relationships with the micro-architecture of soil

Naoise Nunan [a,*], Kejian Wu [b], Iain M. Young [b], John W. Crawford [b], Karl Ritz [c]

[a] *Scottish Crop Research Institute, Plant–Soil Interactions, Invergowrie, Dundee DD2 5DA, UK*
[b] *SIMBIOS Centre, University of Abertay Dundee, Bell Street, Dundee DD1 1HG, UK*
[c] *National Soil Resources Institute, Cranfield University, Silsoe, Bedfordshire MK45 4DT, UK*

Received 5 September 2002; received in revised form 17 December 2002; accepted 19 December 2002

First published online 31 January 2003

Abstract

Biological soil thin-sections and a combination of image analysis and geostatistical tools were used to conduct a detailed investigation into the distribution of bacteria in soil and their relationship with pores. The presence of spatial patterns in the distribution of bacteria was demonstrated at the microscale, with ranges of spatial autocorrelation of 1 mm and below. Bacterial density gradients were found within bacterial patches in topsoil samples and also in one subsoil sample. Bacterial density patches displayed a mosaic of high and low values in the remaining subsoil samples. Anisotropy was detected in the spatial structure of pores, but was not detected in relation to the distribution of bacteria. No marked trend as a function of distance to the nearest pore was observed in bacterial density values in the topsoil, but in the subsoil bacterial density was greatest close to pores and decreased thereafter. Bacterial aggregation was greatest in the cropped topsoil, though no consistent trends were found in the degree of bacterial aggregation as a function of distance to the nearest pore. The implications of the results presented for modelling and predicting bacterial activity in soil are discussed.

Keywords: Spatial patterns; Geostatistics; Soil bacteria; Soil thin sections; Soil structure; Image analysis

1. Introduction

Soil processes related to bacterial activity are often characterised by high intrinsic variability (e.g [1,2]). Spatial variability arises because bacterial communities exist in distinct and different microenvironments within the architecture of the soil, which directly affects their development and activity [3,4]. As a result, accurate quantification of bacterial activity is difficult to achieve and the predictive capacity of models based on known relationships is reduced [5]. Components within ecosystems, however, are not generally distributed in a completely random (i.e. spatially independent) manner, and spatial autocorrelation in community structure can often be detected *at scales relevant to the organisms and communities in question* [6]. Quantification of the spatial variability and identification of appropriate scales can help elucidate the factors driving the development of a particular ecological community, resulting in better predictions of the communities' responses to external factors, and of the effects their activities exert on their environments [5].

Recent research has demonstrated that bacterial communities are not randomly distributed in soil. Spatial patterns have been identified in the distribution of bacteria and bacterial function at scales from several millimetres to several metres [7,8,9] and evidence for bacterial patchiness at scales below 1 mm is now available [9,10]. It has been suggested that microscale spatial patterns may have a regulatory effect on bacterial activity, as a result of the diffusive delivery of substrate to, and the dispersion of product from bacterial cells, which may have rate-limiting or stimulatory effects on microbially mediated processes [10,11]. Furthermore, there is increasing evidence that bacteria can release chemical signals, the environmental concentration of which is related to cell density, that modulate bacterial function once a critical concentration of chemical is reached [12]. This form of regulation is known as quo-

* Corresponding author. Tel.: +44 (1382) 562 731; Fax: +44 (1382) 562 426.
E-mail address: nnunan@scri.sari.ac.uk (N. Nunan).

0168-6496/03/$22.00
doi:10.1016/S0168-6496(03)00027-8

rum-sensing. There is evidence that quorum-sensing occurs in soil (e.g. [13]) and that signalling molecules from non-isogenic bacterial populations can modulate the activity of another population within the wheat rhizosphere microbial community [14]. Thus, the nature of bacterial patches (e.g. relatively large, small, containing a mosaic of regions of high and low cell densities, or density gradients) may also have an impact on a particular function depending on how the supply of substrate, the accumulation of metabolites or signalling molecules affects cells within them.

Soil structure also has regulatory effects on microbial function [15,16]. For example, it has been shown that the response of bacterial communities to substrate addition or to mercury spiking is affected by their location within the soil structure [17,18]. However, the specific location of bacterial populations in relation to other soil features is poorly understood. Random or uniform distributions are usually assumed in studies of microbial function. Rappoldt and Crawford [19] assumed a uniform distribution of respiration in a fractal model of soil when studying the distribution of anoxic volumes. When modelling the effects of cell clustering on ammonium oxidation, Darrah et al. [11] assumed that the clusters of cells were uniformly distributed throughout the soil volume. In a study of the distribution of nitrifier microhabitats in soil, microhabitat aggregates (patches) were simulated around randomly distributed centres [10]. In all cases, the relationship between bacterial populations and the soil structure was not explicitly accounted for.

This study was undertaken to provide a detailed characterisation of the spatial patterns of soil bacterial cells at the microscale (μm to mm) and to determine the nature of the relationship between the cells and pores. Another aim was to derive parameters to inform spatially explicit models of soil bacterial function more accurately. This was achieved using a combination of biological soil thin-sections, image analysis and geostatistical tools. Application of the thin-section technique allows the distribution of soil bacteria to be studied in situ at relevant scales [9,20] and in relation to other soil features such as porosity.

2. Materials and methods

2.1. Soil and sampling

Undisturbed cores (5 cm diameter, 4 cm length) of soil were sampled from the Ap (dark brown sandy silt loam: 71% sand, 19% silt, 10% clay, pH_{H2O} 6.2, 1.9% C and 0.07% N) and B (reddish brown sandy silt loam: 72% sand, 17% silt, 11% clay, pH_{H2O} 6.5, 0.68% C and 0.02% N) horizons of an arable field at the Scottish Crop Research Institute (latitude: 56.46°, longitude: −3.06°). Randomly located samples from the Ap and B horizons were taken in triplicate from a plot (3×3 m^2) that had been fallow for the preceding 2 years. Bacterial abundance heterogeneity in this plot was studied previously at scales ranging from μm to metres [9] and was therefore selected for this more detailed study. Triplicate samples were also taken from the Ap horizon of an adjacent plot (3×3 m^2) directly after harvest of a winter barley (*Hordeum vulgare* L. c.v. Siberia) crop grown under standard agronomic conditions. Sampling in the Ap horizon (topsoil) was at a depth of approximately 5 cm, whilst sampling in the B horizon (subsoil) was at a depth of 62 cm.

2.2. Sample preparation, image acquisition and mapping

Biological thin-sections were produced as described previously [20]. A single randomly oriented thin-section from the horizontal plane was prepared from each core. Thin-sections were mounted on a computer-controlled motorised scanning microscope stage, and 400 (20×20) contiguous RGB digital images in which bacteria could be visualised were acquired using a Zeiss Axioplan 2 microscope fitted for epifluorescence at a magnification of ×630. Bacteria were therefore imaged over an area of 4.51 mm^2 in each thin-section. The location of the first image in each thin-section was chosen at random.

Bacterial numbers and locations (as *xy* coordinates in μm from a reference point situated in the top left hand corner of the first image acquired) were determined in each image using the image processing and analysis procedure described in detail by Nunan et al. [20]. Thin-sections of topsoil samples taken directly after harvest contained bacterial colonies that were not correctly identified using the algorithms described in Nunan et al. [20]. This occurred because these bacteria were often no more than one or two pixels apart, and the edges detected during the edge detection step of the processing procedure merged. In this situation, the bacterial colonies were considered a single feature and often eliminated on the basis of size and/or shape. Furthermore, the edges of the least brightly stained small bacteria were not adequately detected. Therefore the procedure was adapted to account for this: undetected colonies and fainter bacteria were located by encircling them manually in the graphics plane. The graphics plane was then merged with the image plane, producing a binary image in which areas containing undetected bacteria were delimited with rings. The rings were then filled using a binary filling operation. Small bacteria were detected in the blue channel of the RGB image by segmentation after a single smoothing step (highpass filter; filter size: 15×15 pixels). The resultant binary images contained many non-bacterial features, mainly associated with the variable background. Bacteria were distinguished from non-bacterial features after combination with the binary image containing the areas delimited manually as described previously. The bacteria detected in this way were subsequently added to the bacteria detected by the image processing and analysis procedure of Nunan et al. [20] and the *xy* coordinates of all bacterial cells measured. This additional

procedure was applied to all images analysed (cropped topsoil, fallow topsoil and subsoil). Bacterial counts were then made in 61.4×45.9 μm quadrats for geostatistical analysis of bacterial density patterns.

Porosity was mapped at the same locations at which bacterial distributions were measured by acquiring composite RGB images in both transmitted ordinary and cross-polarised light at a magnification of ×100. Binary images of pore and solid space were produced by subtracting images obtained with cross-polarised light from images obtained in ordinary light, and segmenting the resultant images interactively into pore and non-pore space (Zeiss KS300 Imaging System 3.0). Pixel noise was eliminated by removing all features smaller than 20 pixels. Occasionally, due to their orientation or thickness, quartz crystals could not be differentiated from pore space on the basis of spectral properties alone. They were removed manually from the binary image after visual inspection, the decision being based on the fact that quartz crystals have more angular edges. These maps showed pores that were continuous through the section and hence greater than the section thickness of 30–40 μm. The pore maps represented an area of 10.9 mm^2, meaning that pores outside the area in which bacteria were located were also mapped, permitting a more comprehensive analysis of the relationship between pores and bacteria. Bacterial locations within the pore map were determined by overlaying the bacterial images on the pore images using an 'align' function (Zeiss KS300 Imaging System 3.00). The distance between bacterial cells and the nearest pore was determined by applying a 'Euclidean distance transform' to the pore map, and using the distance transform image to label binary bacterial maps. The distance transform produced an image in which each pixel in the solid regions of the original pore map was assigned a greyscale value that was directly related to the distance to the nearest pore. Bacteria in overlaid bacterial maps were then labelled with the greyscale value of the associated pixel in the pore map. Bacteria were thus tagged with a number representing the distance to the nearest pore. Bacteria were then grouped into distance classes with a bin size of 10 μm. Bacterial density (bacterial cell numbers per μm^2) was calculated to account for the differences in area that each distance class represented. The degree of aggregation of the bacterial distributions was estimated by counting the number of neighbours each bacterial cell had within a distance of 20 μm, i.e. the greater the number of neighbours, the greater the degree of aggregation.

2.3. Statistical analysis

Geostatistical analysis is a powerful tool for quantifying spatial patterns based on how sample data are related with distance. Where non-random patterns prevail, spatial autocorrelation can be measured by plotting empirical geostatistical functions (e.g. semivariance or covariance functions). Semivariogram values tend to increase with distance until a plateau (sill) is reached, after which values fluctuate randomly about the sill. The sill represents the total sample variance. The distance at which the sill is reached is called the range and represents the average distance of spatial autocorrelation. Semivariograms usually exhibit a discontinuity at the origin, called the nugget effect (C_0). This is due to variation occurring at scales below the minimum sampling distance and therefore not accounted for, or measurement error. Structural variance (C) is that part of the sample variance which is spatially autocorrelated; hence, the sill is $C+C_0$. Spatial autocorrelation in bacterial patterns and pore space was analysed using the covariance function. Rossi et al. [21] have suggested that the covariance function or covariogram is more appropriate for the study of spatial continuity in ecological samples. The covariogram has the form:

$$C(\boldsymbol{h}) = \frac{1}{N(\boldsymbol{h})}\sum_{i=1}^{N(\boldsymbol{h})}\{[z(x_i)-m_{-\boldsymbol{h}}][z(x_i+\boldsymbol{h})-m_{+\boldsymbol{h}}]\}$$

where $z(x_i)$ and $z(x_i+\boldsymbol{h})$ are two sample values separated by the vector distance $\boldsymbol{h}$, $z(x_i)$ being the tail and $z(x_i+\boldsymbol{h})$ the head of the vector. $N(\boldsymbol{h})$ is the total number of data pairs separated by lag $\boldsymbol{h}$, and $m_{-\boldsymbol{h}}$ and $m_{+\boldsymbol{h}}$ are the means of the values that correspond to the tail and head of the vector, respectively. To allow for comparison between samples, covariograms were standardised by subtracting lag covariance values from the sample covariance and then dividing by the sample covariance. The covariogram was then plotted in semivariogram form and had the same features. The presence or absence of anisotropic structures was investigated using covariograms in the 0°, 45°, 90° and 135° directions; here, 0° represented the x-axis of the bacterial and pore maps. A combination of indicator direct- and cross-semivariograms was used to check for the presence of density gradients in bacterial patches following the concepts of Rivoirard [22] and Webster and Boag [23]. Indicator semivariograms were computed after bacterial density values were coded according to a series of given thresholds (threshold = I): values were coded as zero if the value was below the threshold and 1 if the value was equal to or greater than the threshold. The number of bacterial density values coded as 1 decreased as the threshold increased. Three thresholds were selected for each slide so that the lowest threshold coded approximately 50% of the values as 1, the second threshold 30% and the highest 10%. For two of the subsoil samples the percentages were slightly lower because of the low number of bacteria present. Indicator semivariograms were computed using binary data obtained with a single threshold value and indicator cross-semivariograms were computed using binary data sets generated with two different threshold values. If bacterial density gradients are present and there is a gradual transition from low to high values, then the range of spatial autocorrelation will decrease in the indicator

semivariograms with increasing threshold values. Furthermore, the proportion of spatially autocorrelated variance will increase in the indicator cross-semivariograms. Conversely, if bacterial density values form a mosaic pattern with high and low values randomly dispersed in bacterial patches, then the indicator cross-semivariograms retain their spatial scale and degree of spatial structure with increasing threshold values [22]. All geostatistical analysis was performed using Isatis 4.0.1 (Geovariances, Avon, France).

3. Results

3.1. Bacterial distribution

Bacterial density was greater in the cropped topsoil than in the other soils (Table 1). There were two to five times and 2.6–14 times more bacteria per quadrat in the cropped topsoil than in the fallow topsoil and subsoil, respectively. Extensive variation in the bacterial density between quadrats within soil types was observed in all samples (Table 1). Bacterial density ranged from 0 to 104 cells per quadrat in the cropped topsoil, from 0 to 65 bacteria per quadrat in the fallow topsoil and from 0 to 58 bacteria per quadrat in the subsoil. In the cropped topsoil, 20–29% of the quadrats were devoid of bacterial cells. Equivalent values in the fallow topsoil and the subsoil were 39–65% and 41–69%, respectively. All samples displayed positively skewed distributions, though subsoil samples were more skewed than topsoil samples.

A degree of spatial autocorrelation was observed for all bacterial density distributions (Fig. 1; Table 2). Generally, the range of spatial autocorrelation tended to be greater in the topsoil samples than in the subsoil, though these differences were not statistically significant ($P > 0.05$). The proportion of autocorrelated variance also tended to be greater in the cropped topsoil and least in the subsoil. Nested spherical models were fitted to all experimental semivariograms (e.g. Fig. 1a), except in the case of one fallow topsoil sample and two subsoil samples, to which an exponential model was fitted. Directional covariograms showed that there was little evidence for anisotropic structures in any of the samples (data not shown).

The range of spatial autocorrelation in indicator semivariograms decreased in all topsoil samples (fallow and cropped) and in one of the three subsoil samples as the indicator threshold increased (Fig. 2). The nugget variance, as a proportion of the total sample variance, decreased in the indicator cross-semivariograms for all of these samples also. Indicator semivariograms and indicator cross-semivariograms displayed different trends for the two remaining subsoil samples: cross-indicator semivariograms retained their spatial scale and no trends were observed in indicator semivariograms as the thresholds increased in these two samples (Fig. 3).

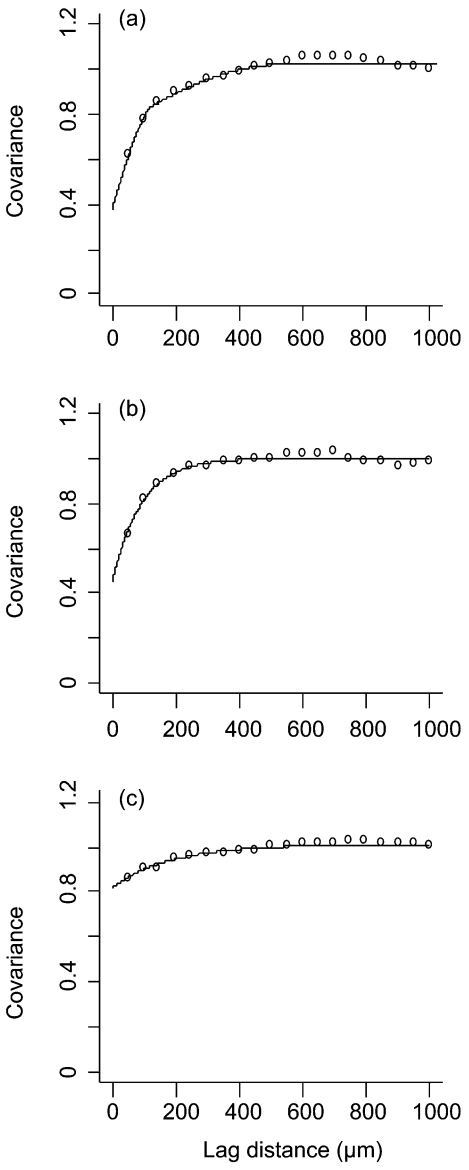

Fig. 1. Examples of standardised covariograms for bacterial density in cropped topsoil (a), fallow topsoil (b) and subsoil (c). Circles are experimental covariograms and lines are models. Exponential models were fitted to covariograms in panels b and c and a double spherical model to the covariogram in panel a.

3.2. Porosity

Porosity measurements were highly variable, both between and within samples (Table 1). Variation between samples was six-fold, two-fold and seven-fold in the cropped topsoil, fallow topsoil and subsoil, respectively. Values tended to be lower in the cropped topsoil. Porosity in quadrats varied between 0 and 100% in all samples and coefficients of variation were always above 100%. A high degree of spatial autocorrelation was observed in all samples, the spatially autocorrelated portion of the variance always accounting for $>80\%$ of the total model variance (Table 2). The range of spatial autocorrelation was correlated with mean porosity values ($r^2 = 0.69$; $P < 0.01$) and

Table 1
Basic statistical summary data for mapped bacterial density and porosity measured in quadrats

Soil	Sample	Bacterial density				Porosity			
		Mean (cells quadrat^{-1})[a]	Median (cells quadrat^{-1})[a]	CV (%)	Skewness	Mean (%)	Median (%)	CV (%)	Skewness
Cropped topsoil	1	7.8	5	119	2.70	2.44	0	428	5.85
	2	8.4	6	111	2.11	15.92	0	198	1.92
	3	6.3	4	118	1.88	14.68	0	205	2.00
Fallow topsoil	1	1.7	0	230	5.51	40.15	2.16	116	0.42
	2	3.3	2	139	2.12	17.76	0	187	1.69
	3	1.9	0	169	2.86	25.39	0	157	1.15
Subsoil	1	0.8	0	240	4.74	5.01	0	294	4.00
	2	0.6	0	200	3.13	38.24	14.33	113	0.67
	3	2.4	1	179	4.36	25.46	3.04	145	1.20

[a]quadrat = 2818 μm^2.

tended to be shorter in the cropped topsoil than in the other two soils. Directional covariograms often showed a degree of anisotropy in that the length of spatial autocorrelation differed between directions (data not shown). However, these differences were not dramatic and were never reflected in bacterial covariograms.

3.3. Relationship between pores and bacteria

In the cropped and fallow topsoil samples, bacterial numbers initially increased and then decreased with distance, whilst maximal bacterial counts were found in the immediate vicinity of pores in the subsoil and declined with distance from the nearest pore (Fig. 4a–c). Bacterial density (cells per μm^2) in the cropped topsoil increased with distance from the nearest pore and tended to remain relatively stable thereafter (Fig. 4d). In the fallow topsoil samples, there was a two- to three-fold increase in bacterial density near pores that was followed by a decrease over distance (Fig. 4e). Bacterial density in the subsoil followed the same pattern as bacterial counts, in that maximal values were found near pores (Fig. 4f).

Aggregation, as measured by the mean number of neighbours within 20 μm of a bacterial cell, was greatest in the cropped topsoil and lowest in the subsoil. The average number of neighbours per cell was 9 in the cropped topsoil, 5 in the fallow topsoil and 3 in the subsoil. There was little evidence of any consistent pattern in relation to transmission pore space (Fig. 4g–i). One of the fallow topsoil samples and one subsoil sample displayed a peak in the number of neighbours at 50–60 μm, whilst another subsoil sample showed a slight decrease in the number of neighbours per cell as the distance to the nearest pore increased (Fig. 4g–i). There were no other consistent or notable trends in aggregation patterns in the remaining samples.

Table 2
Standardised covariogram model parameters for bacterial density and porosity

Soil	Sample number	Bacterial density						Transmission pore space			
		Range per structure (μm)	Total range (μm)	Variance per structure	Nugget variance	Total model variance	Structural variance	Range (μm)	Nugget variance	Total model variance	Structural variance
Topsoil cropped	1	199	1063	0.40	0.43	1.02	0.58	260	0.06	1.00	0.94
		864		0.18							
	2	138	527	0.37	0.38	1.02	0.63	758	0.00	1.04	1.00
		389		0.26							
	3	150	649	0.58	0.31	1.01	0.70	710	0.00	0.99	1.00
		499		0.12							
Topsoil fallow	1	260	941	0.40	0.40	0.96	0.59	1399	0.00	1.15	1.00
		681		0.19							
	2	275	275	0.57	0.43	1.00	0.57	1524	0.06	1.01	0.94
	3	150	758	0.38	0.38	1.00	0.62	1999	0.04	1.23	0.97
		608		0.24							
Subsoil	1	234	234	0.20	0.79	0.99	0.20	355	0.19	1.00	0.81
	2	522	522	0.19	0.82	1.01	0.19	2130	0.07	1.11	0.94
	3	162	466	0.40	0.38	1.01	0.62	1534	0.06	1.06	0.96
		304		0.22							

Range is length of spatial autocorrelation and structural variance is proportion of total model variance that is spatially dependent.

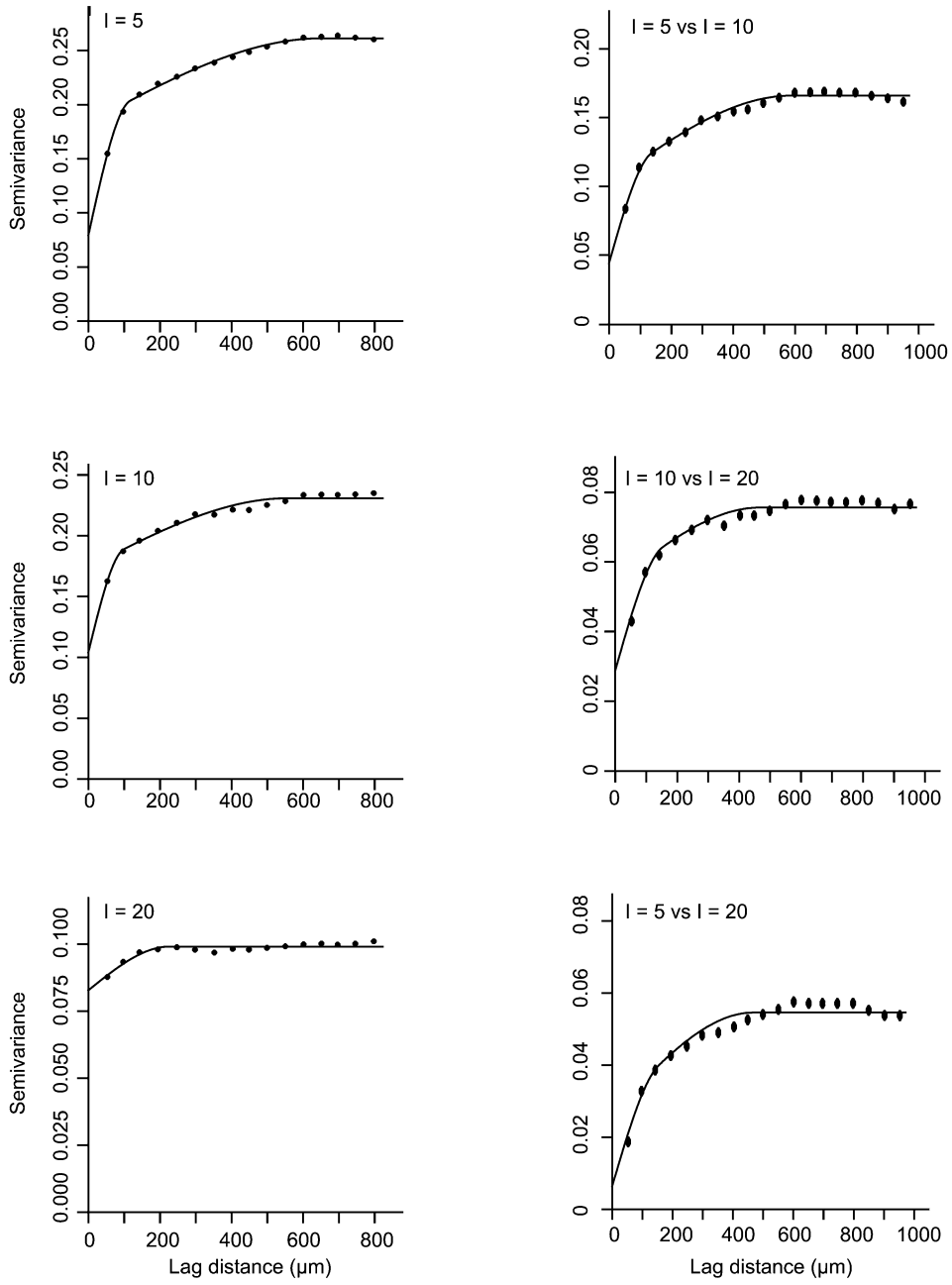

Fig. 2. Example of indicator semivariograms (left) and cross-semivariograms (right) for bacterial density in a cropped topsoil sample, suggesting the presence of gradients. Threshold values (*I*) are indicated in graphs.

4. Discussion

4.1. Bacterial density distribution

Bacterial numbers per quadrat were highly variable and positively skewed (Table 1), confirming the results of Nunan et al. [9]. The latter also found that subsoil samples had larger CVs and were more positively skewed, as was found here. Generally, the rank order of CVs was subsoil > fallow topsoil > cropped topsoil (Table 1), suggesting that bacterial spatial variability was related to the nutrient status of the soil. It may be that when nutrients are rate-limiting, as would be the case in the subsoil and to a lesser extent in the fallow topsoil, bacterial growth is confined to 'pockets' in which nutrients are accessible, hence the greater variability. The range and degree of spatial autocorrelation observed here for fallow topsoil and subsoil samples were consistent with previous results, obtained using a different sampling scheme [9]. The range and structural variance tended to be greatest in the cropped topsoil and lowest in the subsoil, though, contrary to Nunan et al. [9], these differences were not statistically significant.

A short range of spatial autocorrelation coupled with a

skewed frequency distribution for a given variate is indicative of a patchy or 'hot-spot' spatial pattern for that variate [24]. Here, the frequency distributions for bacterial density displayed positive skew (Table 1) and the range of spatial autocorrelation of a number of the sample covariograms was short (Figs. 1b and 2c; Table 2). Furthermore, the sample covariograms with long ranges of spatial autocorrelation were characterised by the presence of nested spherical structures (e.g. Fig. 1a; Table 2) in which the first structure accounted for most of the structural variance and featured a short range. The range of the second structure extended over greater distances but accounted for less of the autocorrelated variance. Thus, these data suggest that soil bacterial communities were present in preferentially colonised patches at the scale of analysis. In a simulation of the spatial distribution of nitrifying micro-organisms in soil, based on the relationship between the percentage of micro-samples (50–500 μm diameter) harbouring nitrifying micro-organisms and the volume of the micro-samples, Grundmann et al. [10] also found a patchy distribution. These results also confirm those of Parkin [25], who found that denitrification was characterised by highly skewed sample frequency distributions and included hot-spots of high specific activity.

4.2. Analysis of bacterial patches

Evidence for bacterial density gradients in patches was found in all six topsoil samples and in one sample from the subsoil (Fig. 2), meaning that regions of high bacterial density were, on average, surrounded by regions of lower bacterial density, and that bacterial density decreased toward the edge of the patch. A plausible explanation for this might be that the gradients were induced by an uneven distribution of organic matter from which soluble compounds were diffusing, with bacterial density greatest close to the organic matter. Gaillard et al. [26] showed that the addition of straw to a soil core induced strong gradients in dehydrogenase activity and in microbial biomass to a distance of 4 mm, and ascribed the gradient to the diffusion of substrate from the straw. In topsoil here, the incorporation of organic matter into the soil during ploughing in previous years and, in the case of the cropped topsoil, rhizodeposition are likely to have had the same effect as the addition of straw to a soil core. Bacterial density gradients were also found in the subsoil sample with the highest bacterial counts, possibly reflecting growth around a nutrient hot-spot due to preferential transport of organic matter down the soil profile. It has been suggested that preferential flow paths have a major effect on the location of biological activity and bacteria in soil. Bundt et al. [27] found differences in the size, composition and activity of microbiological communities within preferential flow paths as compared with the soil matrix and Nunan et al. [9] found spatial structure in the distribution of bacteria at the cm to m scale consistent with spatial structure for water conductivity measurements reported in the literature. Gradients extended over considerably shorter distances here compared with the 4 mm observed in Gaillard et al. [26], as indicated by the ranges of spatial autocorrelation (generally <1 mm), possibly because the substrate sources were less abundant, particularly in the fallow topsoil and subsoil samples.

Visual inspection of bacterial images revealed morphological diversity within patches, especially in the cropped topsoil (Fig. 5b). The ranges of morphotypes (e.g. cocci, rods) and colony morphologies (e.g. chains, sheets) suggest that the genetic diversity and bacterial function might be high at this scale. Franklin et al. [28], using a broad range of analytical methods to study the impact of dilution–regrowth on microbial diversity detected differences in community structure between undiluted and very dilute (10^{-5} and 10^{-6}) samples. Although the overall results suggested a decrease in diversity with dilution, the genetic measures (amplified fragment length polymorphism and terminal restriction fragment length polymorphism) both indicated that a high level of genetic diversity remained in the most dilute samples, providing some corroboration for the observations made here.

A consequence of this type of distribution, in which large numbers of bacterial cells are concentrated in microsites rather than evenly spread, and in which cells are in close proximity to other cells, is that the product of one cell's activity may have an inhibitory or stimulatory effect on the activity of neighbouring cells. Darrah et al. [11] found that a nitrification model accounting for clustering of ammonium-oxidising micro-organisms was better able to reproduce the different time courses of ammonium oxidation reported in the literature than a model based on a uniform cell distribution. This difference was attributed to a lowering of the pH in the microenvironment of bacterial clusters as a result of the nitrification process. Strong et al. [29] provided some corroborating experimental evidence for this. They reported that nitrification became pH-limited at a higher pH in samples treated with lime (to increase the initial pH of the bulk soil) than in control samples. They concluded that the most plausible explanation for the difference was that acid produced during nitrification accumulated in microsites containing nitrifying bacteria, because diffusion into the bulk soil was slow. This meant that pH measurements on bulk soil were not representative of the microenvironment pH experienced by the nitrifying bacteria and so did not give a good indication of when the critical pH for nitrification limitation was reached. Thus, simulation models of nitrification based on pH measurements in bulk soil may not prove to be accurate and may have to consider not only the distribution of micro-organisms but also microscale transport processes. This is likely to be true for microbial processes in soil other than nitrification, such as the biodegradation of pesticides. There is evidence suggesting that certain pesticides are degraded by consortia rather than single strains of

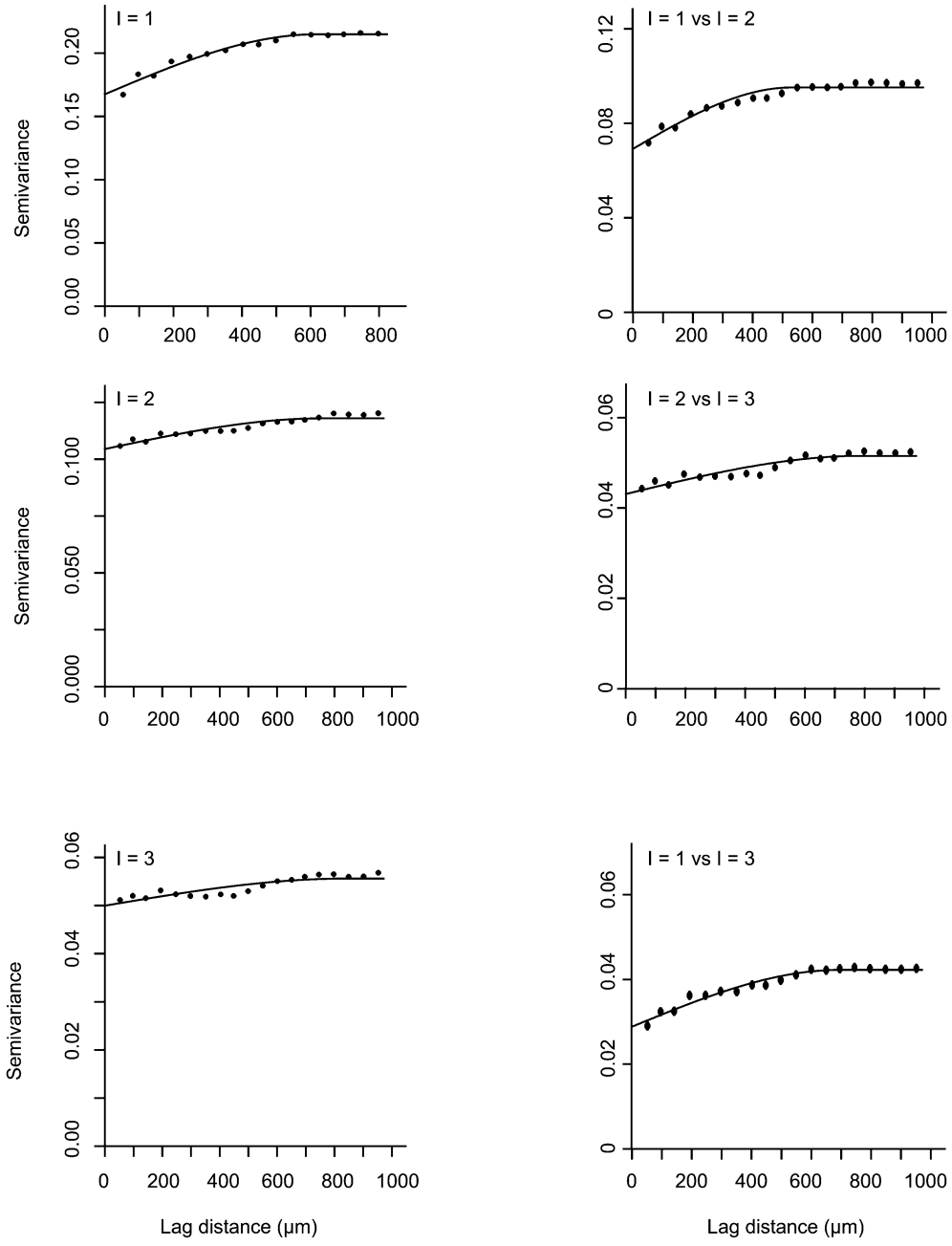

Fig. 3. Example of indicator semivariograms (left) and cross-semivariograms (right) for bacterial density in a subsoil sample, suggesting a mosaic pattern of high and low bacterial density values. Threshold values (*I*) are indicated in graphs.

micro-organisms (e.g. [30]), meaning that for degradation pathways to be complete, intermediate metabolites would have to diffuse from one cell to another. This process would be facilitated if the requisite range of cells tended to exist in close proximity, as is suggested by the observations here. Large concentrations of diverse bacterial populations in microsites would also have consequences if some of the bacterial species exhibited modulation of function via quorum-sensing [12].

Indicator cross-semivariograms suggested a mosaic distribution within the bacterial patches in two of the subsoil samples, with regions of high bacterial density being randomly distributed throughout the bacterial patches (Fig. 3). Therefore, the response of bacterial communities to any local accumulation of inhibitory or stimulatory chemicals may be different in the subsoil to that of bacteria in the topsoil. Similarly, the biodegradation of organic compounds might display different kinetics in subsoil samples if diffusion of intermediate metabolites from one bacterial species to another was rate-limiting.

4.3. Relationship between pores and bacteria

Porosity was more strongly spatially autocorrelated

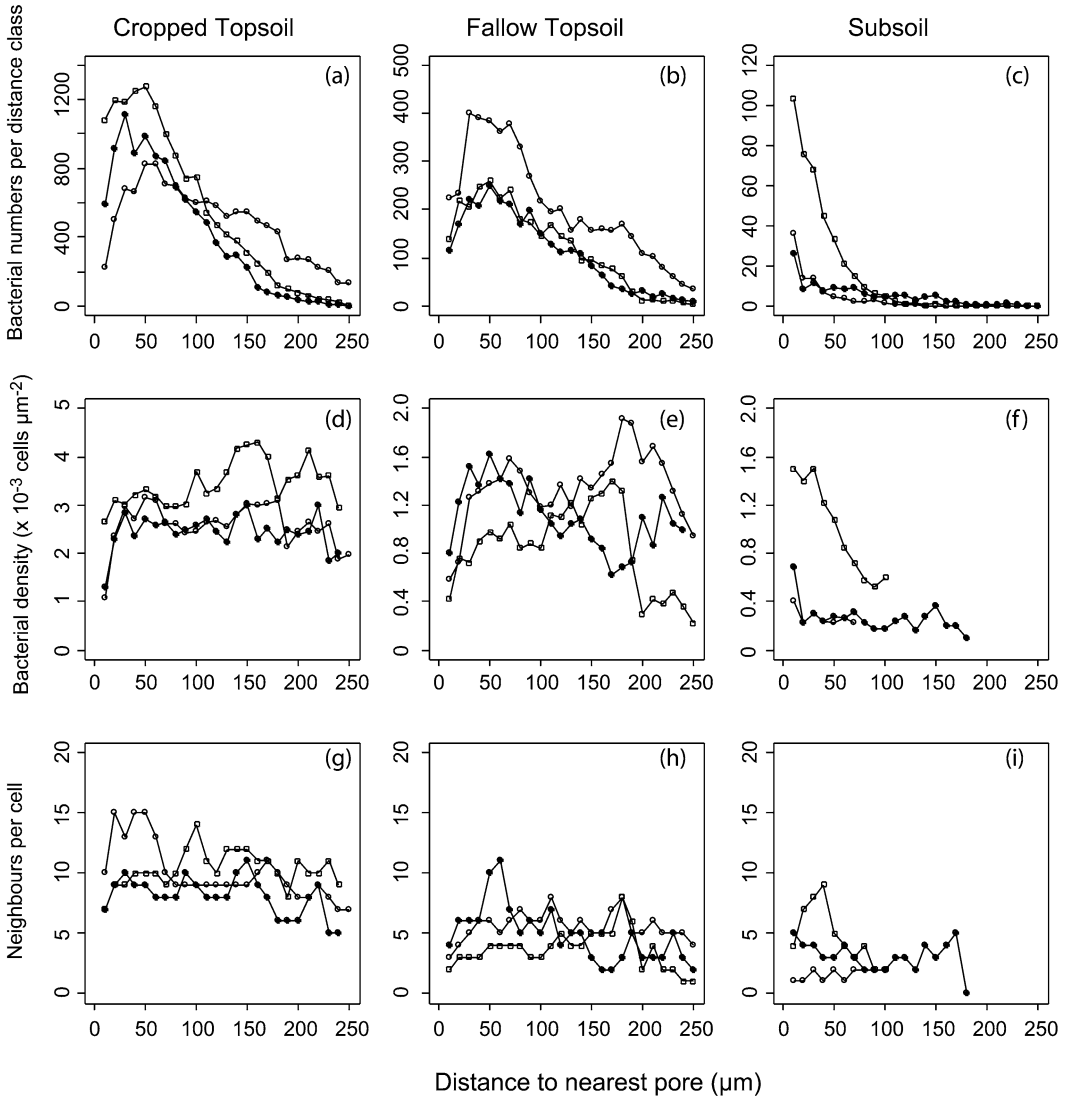

Fig. 4. Bacterial numbers per distance class (a–c), bacterial density (d–f), and average number of neighbours per bacterial cell (g–i) as a function of distance to nearest pore. Bacterial density and neighbour numbers were not calculated at distances where there were no bacteria. Different symbols represent different samples. Note difference in scale of *y*-axes in panels a–f.

than bacterial density (Table 2). Between 81 and 100% of porosity variance in the images was accounted for at this scale, compared with 19–70% in the case of bacterial density. This reflects the fact that the size of pores visible in thin-sections was limited by the thickness of the section (30–40 µm here). Only pores that transmitted through the thin-sections were visible, so variability associated with smaller pores was inevitably filtered out. Directional covariograms suggested that the presence of anisotropic features in porosity did not have an effect on the distribution of bacteria. The delivery of molecules necessary for bacterial growth throughout soil aggregates may be regulated by smaller pores not present in the pore maps and these may have had a more isotropic distribution. However, none of the pore maps were strongly anisotropic and it is possible that if this were the case, then an effect would be seen in the distribution of bacterial cells.

In the topsoil samples, bacterial density was biased away from the immediate vicinity of pores (the first 20 µm) and, in the case of the cropped topsoil, remained relatively stable or increased slightly thereafter (Fig. 4d). In the case of the fallow topsoil, density values fluctuated more widely (Fig. 4e). This is consistent with the findings of Foster [31] and Kilbertus [32] who illustrated with electron micrographs that bacteria were more abundant within aggregates than in larger pores between aggregates. Ranjard et al. [33], using a physical fractionation procedure to separate different soil microenvironments, also concluded that bacterial communities were more abundant within aggregates than outside them. In larger pores, such as the pores in this study, we suggest that the environmental conditions would have been less favourable for the development and persistence of bacterial communities because of (i) more extreme wetting and drying cycles, (ii) leaching of nutrients necessary for growth and (iii) reduced protection from predators [3]. The relatively stable bacte-

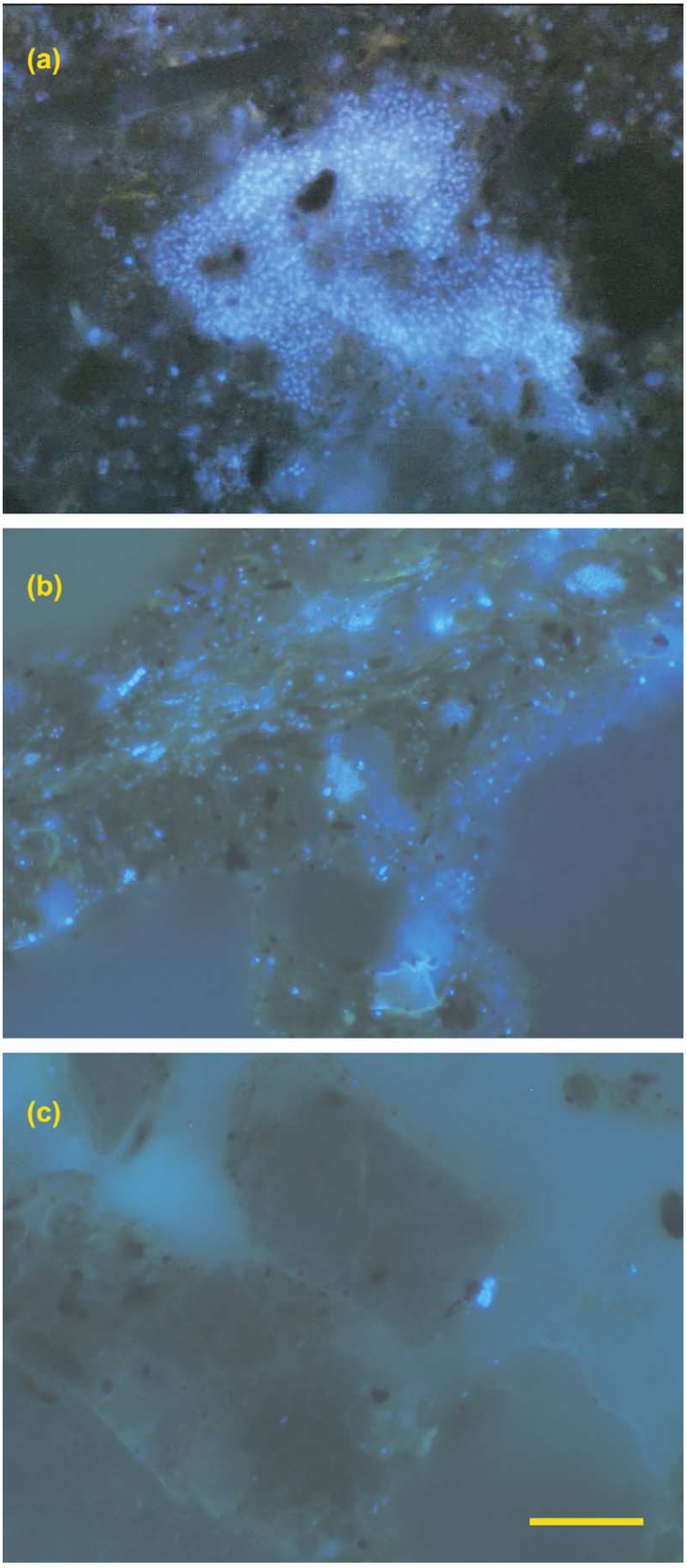

rial density values with distance from pores observed in the cropped topsoil suggest that there was an ample supply of readily available substrate and that this was relatively evenly dispersed. The more variable bacterial density values in the fallow topsoil samples may reflect a more heterogeneous distribution of substrate at the microbial scale, due to a progressive and variable impoverishment of substrate in the system.

The relationship between bacteria and pores in the subsoil was different from that found in the topsoil samples. Here, bacterial density was greatest *close* to pores (Fig. 4f). Substrate would mainly become available to bacterial communities in the subsoil via transport from the topsoil or from roots extending into the subsoil. The relationship between bacterial density and pores was similar for all of the subsoil samples despite the fact that one of the samples was more akin to topsoil in many other respects (bacterial abundance, presence of gradients and degree of spatial structure; Tables 1 and 2; Figs. 3 and 4). This may be a reflection of the location of substrate in the different soils viz. in the vicinity of pores in the subsoil but more randomly dispersed in the topsoil. Spatial associations of bacterial activity and biomass with hot-spots of organic matter have been demonstrated in the past [34,25], albeit at a larger scale, but it may also occur at smaller scales. It is important to have an adequate understanding of the spatial organisation of micro-organisms in relation to pores in structured soil, as problems can occur when trying to relate laboratory measurements on disturbed samples to field-based processes. The results of a study in which the degradation rates of eight pesticides under laboratory and field conditions were compared tend to support this suggestion [35]. No consistent relationship between the two sets of measurements was found and simulations of field degradation rates based on rates measured in the laboratory were inadequate. The authors suggested that sample handling before the laboratory measurements altered the microbial communities and activity, resulting in different degradation rates, as suggested here.

The average number of neighbours within a distance of 20 μm of a bacterial cell was taken as an index of the degree of aggregation in the different bacterial communities, and may also reflect the degree of growth. Bacterial cells in cropped topsoil samples had more neighbours than either fallow topsoil or subsoil samples, suggesting more growth. This would be expected given a greater substrate input to cropped soil. No consistent trend as a function of distance from the nearest pore was found in any of the soils (Fig. 4). The slightly more variable index values as a function of distance in the fallow topsoil compared to the cropped topsoil may be a reflection of a more variable distribution of organic matter, but this is not clear.

As bacterial cells grow by binary fission, the relatively low number of neighbours per cell is quite surprising. However, one should bear in mind that data obtained from thin-sections are a two-dimensional representation of a three-dimensional environment. If we assume that the depth of focus was 1 μm and that the distribution of bacterial cells was isotropic in the three dimensions, then the average number of neighbours per cell within a spherical volume of radius 20 μm would be approximately 27 times greater than the values presented here. However, this calculation does not take account of complex pore geometries that exist in structured soil and which would affect the continuity of the cell mass. This does not sit comfortably with the occasionally expressed view that bacteria exist in soil as biofilms (i.e. large contiguous masses of cells) containing several thousand cells and covering several hundred square micrometres [36,37]. These data suggest that interspecies competition [28], nutrient limitation or both hindered the development of large colonies of morphologically similar cells in unamended arable soil. Fig. 5 shows differences in bacterial colony development in soil with different levels of nutrient limitation. The soil to which readily available substrate, in the form of glucose, was added was found to contain biofilms (Fig. 5a), but this was not the case in either the cropped topsoil or the subsoil (Fig. 5b,c). Whilst biofilms may occur under copiotrophic conditions, where there is an abundance of readily available substrate, the data presented here suggest that they are unlikely to occur in bulk arable soil.

5. Conclusions

This study has demonstrated the presence of spatial autocorrelation in soil bacterial communities at the microscale, i.e. at scales relevant to the communities themselves. The evidence provided strongly suggests that bacteria are found in preferentially colonised patches in soil, located close to pores in the subsoil, but more randomly in topsoil. Bacterial density gradients were detected in patches in topsoil samples and in one of the subsoil samples, but not in the other subsoil samples, suggesting that gradients develop where growth occurs (in the topsoil and in hot-spots in the subsoil). The data suggest that bacterial patches may be associated with local deposits of substrate, but in order to confirm this it would be necessary to develop methods that would allow the distribution of organic matter to be studied at scales similar to that employed in this study. The effects of microbial distribution, both in rela-

←

Fig. 5. Examples of bacterial colonisation of soil; after the addition of glucose (a), in topsoil sampled after harvest (b) and in subsoil (c). Scale bar represents 20 μm. Colonised microsites were generally separated by relatively uncolonised regions, in particular in the subsoil. The image of topsoil (panel b) depicts a relatively densely populated region.

tion to soil structure and in relation to other micro-organisms, have been demonstrated in the past. The relevance and importance of such effects can be studied using this type of methodology in conjunction with associated measurements of microbial function. This would allow a more accurate and complete description of bacterial function in soils and improve the predictive ability of mathematical models.

Acknowledgements

This work was partly funded under the auspices of the UK Department of Trade and Industry LINK Scheme on Biological Treatment of Soil and Water, the Natural Environment Research Council and the Engineering and Physical Sciences Research Council. The Scottish Crop Research Institute receives grant-in-aid from the Scottish Executive Environment and Rural Affairs Department.

References

[1] Bramley, R.G.V. and White, R.E. (1991) An analysis of variability in the activity of nitrifiers in a soil under pasture. 1. Spatially dependent variability and optimum sampling strategy. Aust. J. Soil Res. 29, 95–108.
[2] Cambardella, C.A., Moorman, T.B., Novak, J.M., Parkin, T.P., Karlen, D.L., Turco, R.F. and Konopka, A.E. (1994) Field-scale variability of soil properties in Central Iowa soils. Soil Sci. Soc. Am. J. 58, 1501–1511.
[3] Young, I.M. and Ritz, K. (1998) Can there be a contemporary ecological dimension to soil biology without a habitat? Discussion. Soil Biol. Biochem. 30, 1229–1232.
[4] Ranjard, L. and Richaume, A.S. (2001) Quantitative and qualitative microscale distribution of bacteria in soil. Res. Microbiol. 152, 707–716.
[5] Parkin, T.B. (1993) Spatial variability of microbial processes in soil - a review. J. Environ. Qual. 22, 409–417.
[6] Robertson, G.P. and Gross, K.L. (1994) Assessing the heterogeneity of belowground resources: quantifying pattern and scale. In: Exploitation of Environmental Heterogeneity by Plants: Ecophysiological Processes Above- and Belowground. (Caldwell, M.M. and Pearcy, R.W., Eds.), pp. 237–253. Academic Press, San Diego, CA.
[7] Robertson, G.P., Klingensmith, K.M., Klug, M.J., Paul, E.P., Crum, J.R. and Ellis, B.G. (1997) Soil resources, microbial activity, and primary production across an agricultural ecosystem. Ecol. Appl. 7, 158–170.
[8] Grundmann, G.L. and Debouzie, D. (2000) Geostatistical analysis of the distribution of NH_4^+ and NO_2^--oxidizing bacteria and serotypes at the millimeter scale along a soil transect. FEMS Microbiol. Ecol. 34, 57–62.
[9] Nunan, N., Wu, K.J., Young, I.M., Crawford, J.W. and Ritz, K. (2002) In situ spatial patterns of soil bacterial populations, mapped at multiple scales, in an arable soil. Microb. Ecol. 44, 296–305.
[10] Grundmann, G.L., Dechesne, A., Bartoli, F., Flandrois, J.P., Chasse, J.L. and Kizungu, R. (2001) Spatial modeling of nitrifier microhabitats in soil. Soil Sci. Soc. Am. J. 65, 1709–1716.
[11] Darrah, P.R., White, R.E. and Nye, P.H. (1987) A theoretical consideration of the implications of cell clustering for the prediction of nitrification in soil. Plant Soil 99, 387–400.
[12] Whitehead, N.A., Barnard, A.M.L., Slater, H., Simpson, N.J.L. and Salmond, G.P.C. (2001) Quorum-sensing in gram-negative bacteria. FEMS Microbiol. Rev. 25, 365–404.
[13] Pierson, L.S., Keppenne, V.D. and Wood, D.W. (1994) Phenazine antibiotic biosynthesis in Pseudomonas-Aureofaciens-30-84 is regulated by Phzr in response to cell-density. J. Bacteriol. 176, 3966–3974.
[14] Pierson, E.A., Wood, D.W., Cannon, J.A., Blachere, F.M. and Pierson, L.S. (1998) Interpopulation signaling via N-acyl-homoserine lactones among bacteria in the wheat rhizosphere. Mol. Plant Microbe Interact. 11, 1078–1084.
[15] Vanveen, J.A. and Kuikman, P.J. (1990) Soil structural aspects of decomposition of organic-matter by microorganisms. Biogeochemistry 11, 213–233.
[16] Young, I.M. and Ritz, K. (2000) Tillage, habitat space and function of soil microbes. Soil Till. Res. 53, 201–213.
[17] Chenu, C., Hassink, J. and Bloem, J. (2001) Short-term changes in the spatial distribution of microorganisms in soil aggregates as affected by glucose addition. Biol. Fertil. Soils 34, 349–356.
[18] Ranjard, L., Nazaret, S., Gourbiere, F., Thioulouse, J., Linet, P. and Richaume, A. (2000) A soil microscale study to reveal the heterogeneity of Hg(II) impact on indigenous bacteria by quantification of adapted phenotypes and analysis of community DNA fingerprints. FEMS Microbiol. Ecol. 31, 107–115.
[19] Rappoldt, C. and Crawford, J.W. (1999) The distribution of anoxic volume in a fractal model of soil. Geoderma 88, 329–347.
[20] Nunan, N., Ritz, K., Crabb, D., Harris, K., Wu, K.J., Crawford, J.W. and Young, I.M. (2001) Quantification of the in situ distribution of soil bacteria by large-scale imaging of thin sections of undisturbed soil. FEMS Microbiol. Ecol. 37, 67–77.
[21] Rossi, R.E., Mulla, D.J., Journel, A.G. and Franz, E.H. (1992) Geostatistical tools for modeling and interpreting ecological spatial dependence. Ecol. Mon. 62, 277–314.
[22] Rivoirard, J. (1994) Introduction to Disjunctive Kriging and Nonlinear Geostatistics. Clarendon Press, Oxford.
[23] Webster, R. and Boag, B. (1992) Geostatistical analysis of cyst nematodes in soil. J. Soil Sci. 43, 583–595.
[24] Robertson, G.P., Crum, J.R. and Ellis, B.G. (1993) The spatial variability of soil resources following long-term disturbance. Oecologia 96, 451–456.
[25] Parkin, T.B. (1987) Soil microsites as a source of denitrification variability. Soil Sci. Soc. Am. J. 51, 1194–1199.
[26] Gaillard, V., Chenu, C., Recous, S. and Richard, G. (1999) Carbon, nitrogen and microbial gradients induced by plant residues decomposing in soil. Eur. J. Soil Sci. 50, 567–578.
[27] Bundt, M., Widmer, F., Pesaro, M., Zeyer, J. and Blaser, P. (2001) Preferential flow paths: biological 'hot spots' in soils. Soil Biol. Biochem. 33, 729–738.
[28] Franklin, R.B., Garland, J.L., Bolster, C.H. and Mills, A.L. (2001) Impact of dilution on microbial community structure and functional potential: Comparison of numerical simulations and batch culture experiments. Appl. Environ. Microbiol. 67, 702–712.
[29] Strong, D.T., Sale, P.W.G. and Helyar, K.R. (1997) Initial soil pH affects the pH at which nitrification ceases due to self-induced acidification of microbial microsites. Aust. J. Soil Res. 35, 565–570.
[30] Ou, L.T. and Thomas, J.E. (1994) Influence of soil organic-matter and soil surfaces on a bacterial consortium that mineralizes Fenamiphos. Soil Sci. Soc. Am. J. 58, 1148–1153.
[31] Foster, R.C. (1988) Microenvironments of soil-microorganisms. Biol. Fertil. Soils 6, 189–203.
[32] Kilbertus, G. (1980) Study of microhabitats in soil aggregates - Relation to bacterial biomass and size of procaryotes. Rev. Ecol. Biol. Sol 17, 543–557.
[33] Ranjard, L., Poly, F., Combrisson, J., Richaume, A., Gourbiere, F., Thioulouse, J. and Nazaret, S. (2000) Heterogeneous cell density and genetic structure of bacterial pools associated with various soil microenvironments as determined by enumeration and DNA fingerprinting approach (RISA). Microb. Ecol. 39, 263–272.
[34] Ronn, R., Griffiths, B.S., Ekelund, F. and Christensen, S. (1996)

Spatial distribution and successional pattern of microbial activity and micro-faunal populations on decomposing barley roots. J. Appl. Ecol. 33, 662–672.
[35] Di, H.J., Aylmore, L.A.G. and Kookana, R.S. (1998) Degradation rates of eight pesticides in surface and subsurface soils under laboratory and field conditions. Soil Sci. 163, 404–411.
[36] Harris, P.J. (1994) Consequences of the spatial distribution of microbial communities in soil. In: Beyond the Biomass (Ritz, K., Dighton, J. and Giller, K.E., Eds.), pp. 239–246. British Society of Soil Science, Wiles-Sayce, Chichester.
[37] Chappell, M.A. and Evangelou, V.P. (2002) Surface chemistry and function of microbial biofilms. Adv. Agron. 76, 199.